SIMULATION STUDY ON THE VARIATION PATTERN OF TOOL-CHIP CONTACT LENGTH IN THE BTA DEEP-HOLE DRILLING PROCESS

Bian GUO[1,a], Yan LI[2], Jianming ZHENG[2], Luo YANG[2], Xubo LI[2] and Li LIU[1]

ABSTRACT: In the metal cutting process, tool-chip contact length directly affects the chip deformation, cutting temperature distribution and tool wear. We use the DEFORM-3D finite element analysis software to simulate the drilling process of a staggered teeth BTA drill, analyze the chip formation process, deformation pattern of each cutting tooth of the staggered teeth BTA drill and study the variation pattern of the tool-chip contact length with the cutting speed and feed during the drilling process of 45 steel and 20CrMnMo. The results show that the tool-chip contact length of each cutting tooth of the BTA drill is different and that the tool-chip contact length increases with the decrease of the material strength and the cutting speed and increases with the increase of the feed. We verify the reliability of the finite element simulation by comparing the cutting force simulation data with the cutting force experimental data.
KEY WORDS: tool-chip contact length, staggered teeth BTA drill bit, cutting force, FEM simulation.

1 INTRODUCTION

Deep-hole machining is a difficult, technically demanding and costly machining technology. With the development of precision machining, higher requirements have been raised for the deep-hole drilling process and technology, prompting researchers to further study this technology (Biermann et al., 2011). In the metal cutting process, tool-chip contact length directly affects chip deformation, cutting temperature, tool wear and machined surface quality (Liu, 1998). At present, researches on tool-chip contact length at home and abroad mainly focus on how to use a geometric model to calculate the tool-chip contact length and its relationship with the cutting force. Ucun, et al. (2009) studied the variation pattern of tool-chip contact length in the orthogonal metal cutting process and the results show that feed increase and different workpiece materials have very important effects on the tool-chip contact length. Korkut and Donertas (2007) studied the effects of feed and cutting speed on the cutting force, surface roughness and tool-chip contact length in the end milling process and the results show that the cutting force increases with the increase of feed and cutting thickness. Liu (1998) explored the effects of tool-chip contact length on chip deformation through cutting experiments and the results show that tool-chip contact length is a substantial internal factor that affects chip deformation while the strength of workpiece material, tool orthogonal rake, cutting speed and feed are the external factors to chip deformation. Wan and Liu (2002) found through cutting tests that when the tool-chip contact length of the rake face of the tool decreases, the cutting force shows a nonlinear decrease. However, few of the previous studies addressed the contact characteristics of the tool-chip interface in BTA deep-hole drilling. In this paper, we use the finite element analysis software DEFORM-3D to establish the BTA deep-hole drilling model, analyze the tool-chip contact of each cutting tooth and the cutting force, study the pattern of how the tool-chip contact length varies with the cutting parameters. We verify the reliability of the finite element simulation by the BTA deep hole drilling experiment.

[1] School of Mechanical Engineering, Baoji University of Arts and Sciences, Baoji 721016, China

[2]School of Mechanical and Precision Instrument Engineering, Xi'an University of Technology, Xi'an 710048, China

E-mail: [a]gguo2006@126.com

2 PRINCIPLE OF BTA DEEP-HOLE DRILLING AND DRILL GEOMETRIC MODEL

2.1 Principle of BTA deep-hole drilling

The operating principle of BTA deep-hole drilling is shown in Figure 1. BTA deep-hole machining system uses the inner-chip removal method. The drill bit is installed on the hollow drill pipe. It makes high-speed rotation and feed movements relative to the workpiece. The high

pressure cutting oil enters the cutting zone via the oil supply machine and the gap between the bore wall of the workpiece and the outer surface of the drill pipe to complete the cooling and lubrication of the drill bit and then discharges the chip generated during the drilling process backwards via the chip removal channel and the drill pipe bore to the chip tray. The cutting fluid returns to the oil tank via the strainer and is then pumped out by the oil feed pump for reuse after being filtered for several times. In this way, the deep-hole drilling is maintained highly-efficient and continuous.

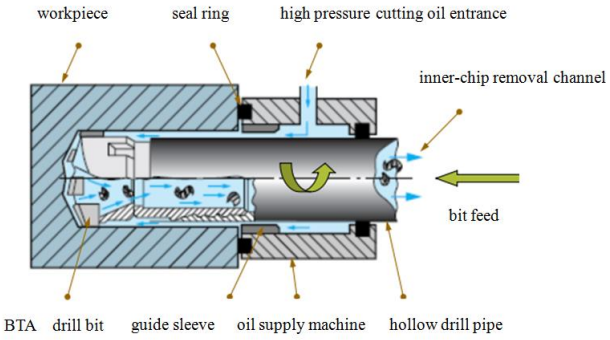

Figure 1. Operating principle of the BTA deep-hole machining system

2.2 Geometric model for the BTA drill

A BTA drill is usually designed to have a staggered-tooth structure with three cutting teeth, two guide bars and two chip removal channels. The two guide bars and the outer cutting edge compose three points that can fix a circle and thus achieves self-steering in the cutting process (Richardson and Bhatti, 2011). We use SolidWorks to build a 3D solid model for the staggered teeth BTA deep-hole drill bit, as shown in Figure 2, where the diameter is φ17.73mm, the outer tooth width 3.865mm, the middle tooth width 2.5mm, the inner tooth width 3.5mm, the deflection angle of the outer tooth 13°, the deflection angle of the middle tooth 13° and the deflection angle of the inner tooth 18°.

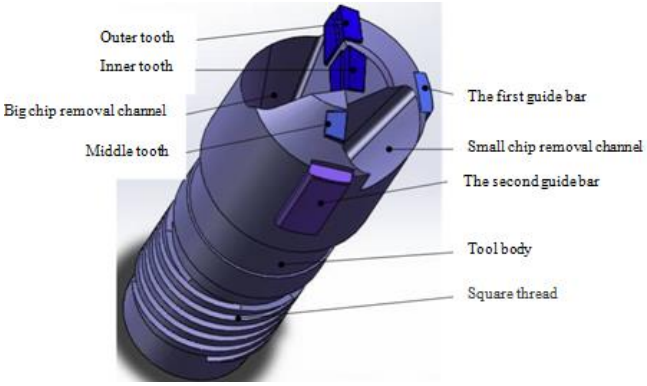

Figure 2. Graphic model of staggered teeth BTA drill

3 FINITE ELEMENT SIMULATION MODEL FOR BTA DEEP-HOLE DRILLING

3.1 Modeling and grid division of BTA deep-hole drilling

The workpiece modeling in this paper follows the "simplest" principle, that is, to simplify the workpiece as much as possible as long as it can reflect the cutting conditions. In order to save drilling time, we ignore the initial penetration stage in actual drilling and directly start our simulation from the middle of the drilling process. Therefore, the workpiece model needs to completely match the tool, including the widths and cutting edge angles of the three cutting teeth of the staggered teeth BTA drill. In this paper, the simulated workpiece model is shown in Figure 3, with a size of Φ17.73 × 7mm and a pre-drilling depth of 3mm.

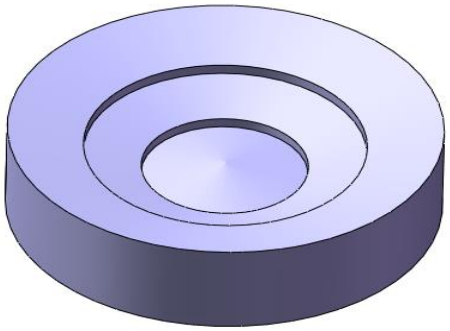

Figure 3. Graphic model of workpiece

In the finite element simulation of the cutting process, grid division is very important to the simulation precision and computation amount. To avoid unqualified and distorted grid cells, we use the adaptive meshing technology for grid division (Fang & Zeng, 2003). In this paper, we set the workpiece as a plastic body and adopt the absolute cell type, where the ratio is 4, the total number of cells is around 220812 and the length of the minimum cell of the workpiece is slightly smaller than the feed. We encrypt the local cutting zone, set the grids to be re-divided with the tool movement; the drill bit is set as a rigid body, where the ratio is set to 7, the total number of cells is 28086 or so and the relative cell type is adopted. The grid division results of the drill bit and the workpiece are shown in Figure 4.

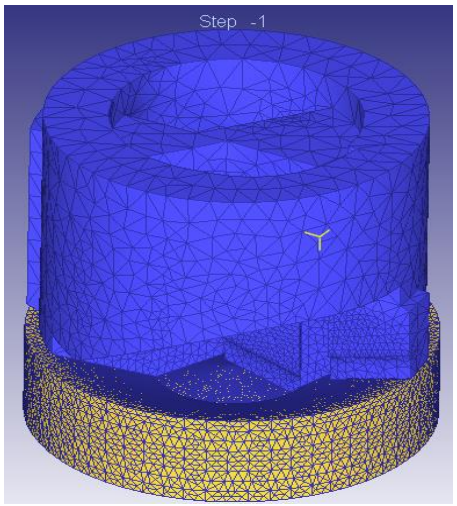

Figure 4. Finite element simulation model and grid division

3.2 Material constitutive model

In the finite element simulation model of the cutting process, the constitutive model of the workpiece material is the basis for material failure determination. Currently, the most commonly used one is the Johnson-Cook model, which is a constitutive model suitable for large deformation, high strain and high-temperature deformation (Cai et al., 2009). In this paper, we choose the Johnson-Cook model as the constitutive model of the workpiece material, whose expression is (Samantaray et al., 2009):

$$\sigma = (A + B\varepsilon^{n})(1 + C\ln\dot{\varepsilon})(1 - T^{*m}) \quad (1)$$

Where, σ is the true stress (following the Von Mises yield criterion); A is the yield stress of the material at a specific temperature and strain rate; B is the strain hardening coefficient; ε is the equivalent plastic strain; n is the strain hardening exponent; C is the strain-rate sensitivity; $\dot{\varepsilon}$ is the dimensionless strain rate; T^* is the dimensionless temperature, $T^*=(T-Tr)/(Tm-Tr)$, where Tr is the reference thermodynamic temperature; Tm is the thermodynamic temperature of the melting point; m is the temperature sensitivity coefficient. We assume that the material is isotropic, and A, B, C, n and m can all be obtained from experiments. The Johnson-Cook model parameters of 45 steel and 20CrMnMo steel are shown in Table 1(Chen et al., 2007).

Table 1. The Johnson-Cook model parameters of 45 steel and 20CrMnMo steel

Material	A	B	n	m	Tm/K	Tr/K
45 steel	506	320	0.28	1.06	1723	298
20CrMnMo steel	626	347	0.48	0.61	1800	188

3.3 Model materials and parameter setting

In the simulation, the basic physical properties of the tool material WC based cemented carbide and the workpiece materials AISI-1045 (45 steel) and 20CrMnMo are shown in Table 2.

Table 2. The physical properties of WC cemented carbide inserts and workpiece material

Material	Young modulus(GPa)	Poisson ratio	Thermal conductivity(W/m/°C)	Heat capacity (N/mm2/°C)	Thermal expansion coefficient (10.6/°C)
WC cemented carbide inserts	650	0.25	59	15	5
45 steel	215	0.3	41.7	3.61	10.1
20CrMnMo steel	198	0.254	35	3.15	9.5

In this paper, we set the tool as the main piece and the workpiece as the accessory piece. The contact tolerance is 0.00305mm; the friction between the tool and the workpiece is defined as the shearing friction, with the coefficient being 0.6. In the actual deep hole drilling process, the cooling fluid with certain pressure and flow is supplied. In order to simulate the cooling and lubrication conditions of the processing environment, we set the ambient temperature is -10°C and the thermal conductivity coefficient is 0.06 N/sec/mm/°C.

3.4 Selection of the tool wear model

In the simulation process, we use the Usui model to simulate tool wear. The calculation formula for tool wear is (Shirakashi & Usui, 1976):

$$\sigma = \int apve^{-b/T}dt \quad (2)$$

Where, σ is wearing depth; p is positive pressure of the contact surface; v is sliding speed of

the workpiece relative to the tool; *dt* is time increment; T is contact surface temperature; a, b are test coefficient, often set as a=0.0000001 and b=855.

3.5 Setting of boundary conditions

When setting the movement relations between the drill bit and the workpiece, we impose full constraint on the workpiece to fix it and set the drill bit to rotate and feed along the Z-axis.

4 SIMULATION RESULTS AND ANALYSIS OF BTA DEEP-HOLE DRILLING

4.1 Chip formation process and variation patterns

By using the simulation model, we simulate the drilling process of the workpiece made of 45 steel at a feed rate of 0.1mm/r and a rotating speed of 720r/min. The chip formation process and the three deformation zones are shown in Figure 5. It can be seen that the simulation results are in good agreement with the actual field machining process. During the whole drilling process, the tool contacts, extrudes and rubs against with the workpiece, forming three typical deformation zones. The metal material of the part cut off in the basic deformation area separates from the workpiece and form chip after severe shear slip; under the action of positive pressure and friction force, the interface between the bottom layer of the chip and the rake face of the tool is subjected to plastic deformation and form the second deformation zone, and the third deformation zone is located where the chip separates from the workpiece body. There, the flank surface of the tool extrudes and rubs against with the machined surface of the workpiece, which results in deformation, and produces residual stress and work hardening.

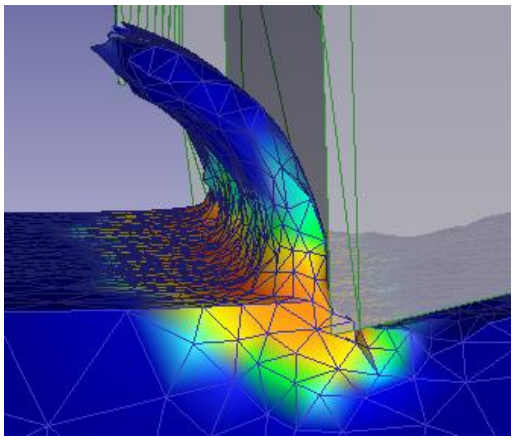

Figure 5. The simulation results of chips forming process

From the simulated drilling process, it can be found that from the geometric center of the drill bit to the outer circle, the drilling conditions vary greatly. Therefore, the cutting forms and patterns of the three cutting teeth of the BTA drill are different during the drilling process, as shown in Figure 6.

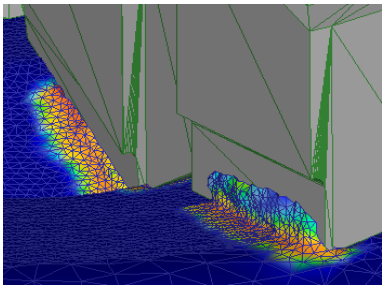

t =0.0021s

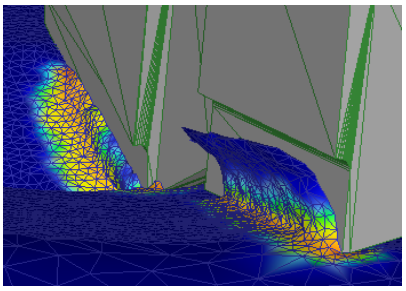

t =0.012s

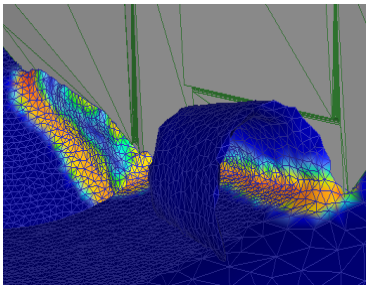

t =0.029s

(a) The chip formation process of the outer and the inner cutting tooth

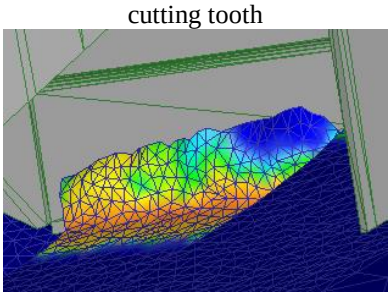

t =0.0021s

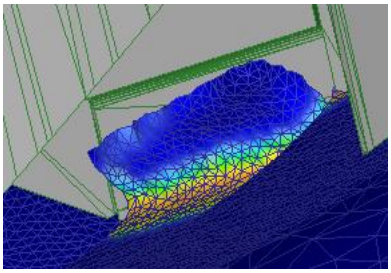

t =0.012s

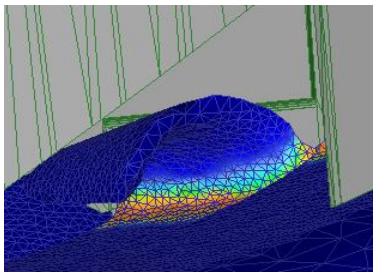

t =0.029s

(b) The chip formation process of the middle cutting tooth

Figure 6. Chip formation process of each cutting tooth when the BTA drill is used to drill 45 steel.

It can be seen from the simulated cutting process of the middle tooth in Fig.6(b) that, as the cutting progresses, the stress at the contact between the workpiece and the blade continuously increases, and plastic yield begins after 0.0021s. When the yield stress reaches the chip separation criterion, the contact separates, forming chip. With the cutting continuing, the contact area between the rake face of the tool and the chip keeps increasing. At 0.012s, the chip separates from the rake face, and starts to bend; at 0.029s, the whole chip formation process is basically completed, forming C-shaped chip.

Comparing the simulated cutting processes of the three cutting teeth, as shown in Fig. 6 (a) and (b), we can see that with the decrease of the workpiece radius, the cutting speed and the curvature radius of the workpiece gradually decrease and the cutting conditions for the cutting teeth are significantly changed. For the outer tooth, the cutting speed and the curvature radius of the workpiece are the largest, so the cutting conditions are the best, which can help form chip easily and result in relatively small deformation. In addition, the contact between the chip and the rake surface of the tool has the greatest length and the largest area. With the cutting speed and the curvature radius of the workpiece gradually decreasing, the cutting conditions worsen gradually and the chip deformation gets more severe. It is more difficult to form chip and the extrusion deformation becomes more serious.

4.2 Variation patterns of tool-chip contact length

The tool-chip contact length lc is the length of the section from the bottom of the chip when it begins to flow out to the point when it separates from the rake face, as shown in Figure 7. During measurement, we select 8 groups of equidistant nodes on the tool contact surface, i.e. the rake face. There are certain deviations in the measurement, so we finally take the average value of the measured data as the tool-chip contact length *lc*(mm).

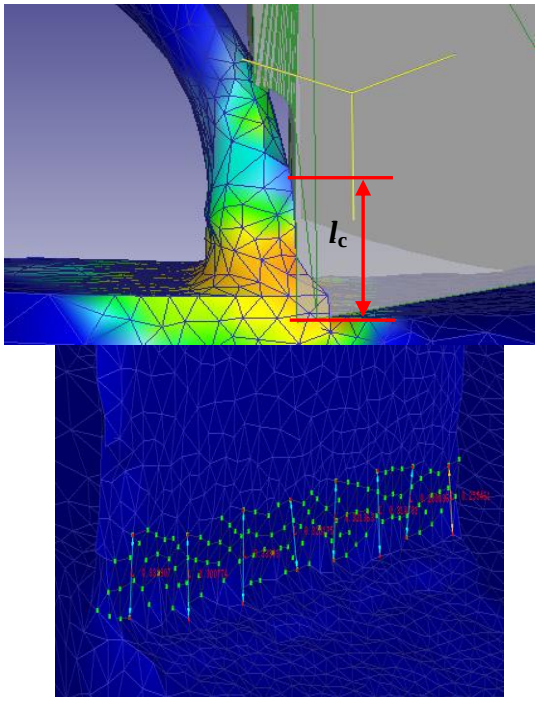

Figure 7. The length measurement chart of the tool-chip contact

In the above simulation model, we change the feed, main shaft speed and workpiece material and measure the tool-chip contact length for each cutting tooth under different working conditions. The workpiece 45 steel is denoted as M1 and 20CrMnMo as M2. The tool-chip contact lengths for each cutting tooth of the BTA drill under different cutting parameters are shown in Figure 8 and 9.

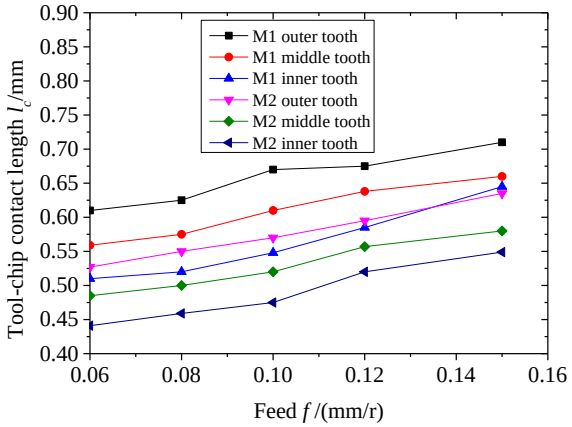

Figure 8. Tool-chip contact length *lc* vs. feed *f*

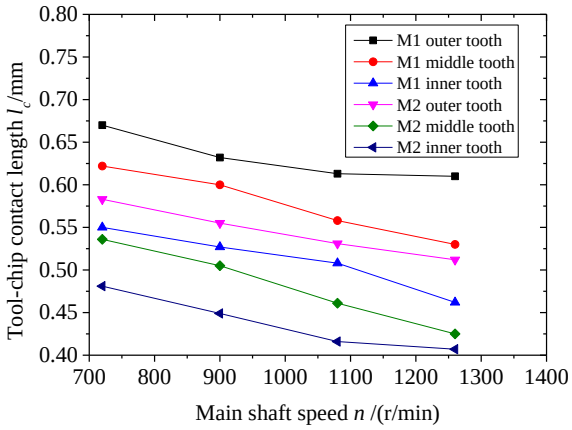

Figure 9. Tool-chip contact length *lc* vs. main shaft speed *n*

By analyzing Figure 8 and 9, we can conclude:

(1) When the cutting speed is constant (n=720r/min), as the feed increases, the tool-chip contact length lc increases for different materials. This is because when the feed increases, the thickness of the cutting layer also increases, making the chip not easily curled and close to the rake face until it starts plastic deformation under the secondary action of the chip breaker. As a result, the tool-chip contact length is increased.

(2) When the feed is consistant (f=0.1mm/r), as the main shaft speed, i.e. the cutting speed increases, the tool-chip contact length lc decreases regardless of the material, because the greater the cutting speed is, the more curly the chip is, and the smaller the curvature radius is. In this way, the chip can separate from the rake face of the tool more quickly, making the tool-chip contact length lc smaller.

(3) When the cutting speed and the feed are constant, the tool-chip contact length lc gradually increases from the drill geometric center to the outer circle, which means, the tool-chip contact area for the rake face of the outer tooth is the largest. Regarding the materials, the tool-chip contact length lc of each cutting tooth for 20CrMnMo is less than that for 45 steel, which shows that with the increase in material strength, the tool-chip contact length is reduced.

5 EXPERIMENTAL STUDY ON CUTTING FORCE OF BTA DEEP HOLE DRILLING

5.1 Experimental system

The deep hole drilling experimental system mainly consists of two parts, one is the machine tool equipment and the cutting force measuring system, and the other is the acquisition system, as shown in Figure 10.

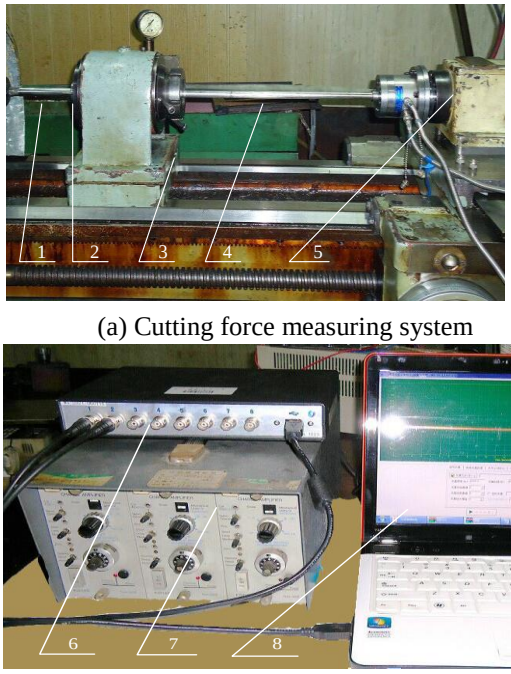

(a) Cutting force measuring system

(b) Acquisition system

Figure 10. The deep hole drilling experimental system

Where, 1 is workpiece; 2 is BTA drilling bit; 3 is steady rest; 4 is drill pipe; 5 is dynamometer; 6 is data acquisition card; 7 is charge amplifier; 8 is computer.

5.2 Comparison of cutting force experiment results with simulation results

We compare cutting force experimental data and simulation data when the spindle speed n is 900 r/min during the drilling process of 20CrMnMo in Figure 11 and during the drilling process of 45 steel in Figure 12.

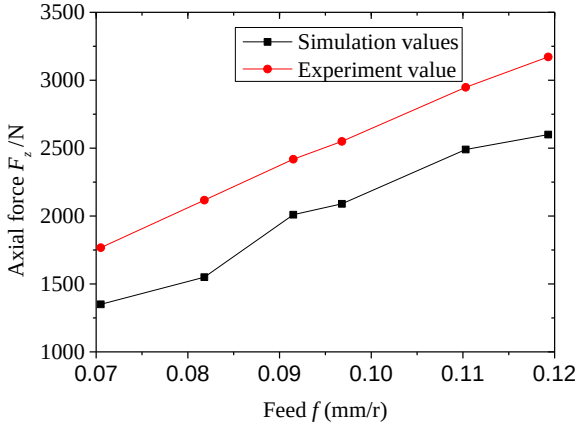

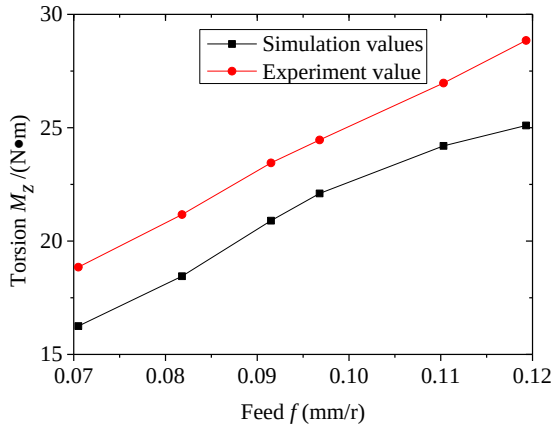

Figure 11. Cutting force comparison of 20CrMnMo

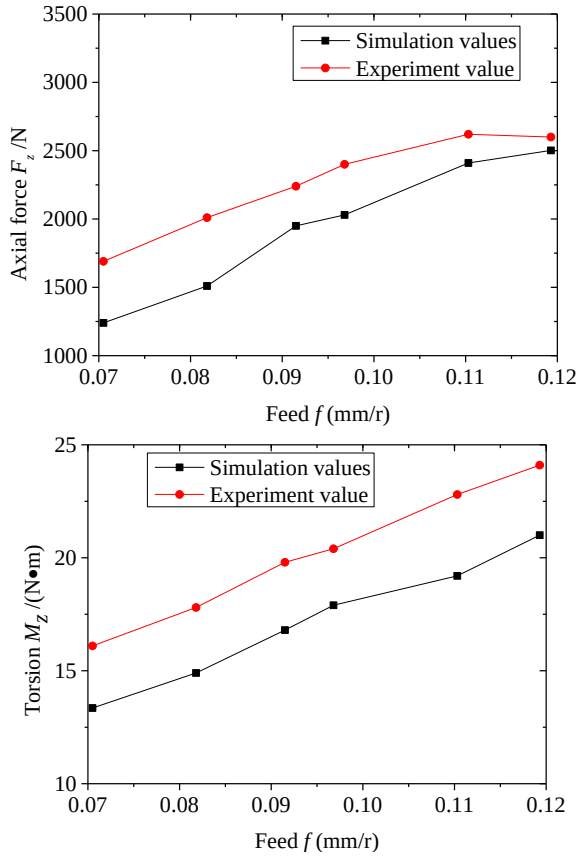

Figure 12. Cutting force comparison of 45 steel

It can be seen from cutting force comparison in Figure 11 and Figure 12 that the cutting force simulation value is slightly less than the experimental value, there are the same trend between the two. This is because the simulation model has a certain simplification, without considering the force of the guide bar.

6 CONCLUDING REMARKS

We use the finite element software DEFORM-3D to establish a staggered BTA drilling simulation model and dynamically simulate the cutting process of each cutting tooth of the staggered teeth BTA drill. In this way, we obtain the cutting deformation processes and the tool-chip contact lengths of the three cutting teeth in the drilling process. According to the results, the tool-chip contact length of each cutting tooth of the staggered teeth BTA drill is different – it gradually increases from the inner tooth to the outer tooth; at the same time, under different cutting parameters, the tool-chip contact length varies. As the material strength and cutting speed decrease and the feed increases, the tool-chip contact *lc* increases. The reliability of the simulation is verified by BTA deep hole drilling experiment.

7 ACKNOWLEDGEMENTS

The author gratefully acknowledges the Science and Technology Program of China's Shaanxi Province (Industrial Key Technologies R&D Program, Grant, No. 2013K08-14), the Education Department of China's Shaanxi Provincial Government (Science and Technology Development Plan, Grant, No. 16JK1041, 16JK1044), the Science and Technology Program of Baoji University of Arts and Sciences (No. ZK16006), undergraduate innovative entrepreneurship training program (201510721616, 2049) for the research grant.

8 REFERENCES

►Biermann, D., Heilmann, M., Kirschner, M. (2011). *Analysis of the Influence of Tool Geometry on Surface Integrity in Single-lip Deep Hole Drilling with Small Diameters.* Procedia Engineering, 19: 16-21.

►Cai, Y.J., Duan, C.Z., Li Y.Y., et al. (2009). *FE simulation of chip formation during high speed machining based on ABAQUS.* Journal of Mechanical Strength, 31(4): 693-696.

►Chen, G., Chen, X.W., Chen, Z.F., et al. (2007). *Simulations of A3 steel blunt projectiles impacting 45 steel plates.* Explosion and Shock Waves, 27(5): 390-397.

►Fang, G., Zeng, P. (2003). *FEM simulation of orthogonal metal cutting process.* Mechanical Science of Technology, 22(4): 641-645.

►Korkut, I., Donertas, M.A. (2007). *The influence of feed rate and cutting speed on the cutting forces, surface roughness and tool-chip length during face milling.* Materials and Design, 28: 308-312.

►Liu H. (1998). *Influence of tool-chip contact length on chip deformation.* Journal of Baotou University of Iron and Steel Technology, 17(1): 36-39.

►Richardson, R., Bhatti, R. (2011). *A review of research into the role of guide pads in BTA deep*

hole machining. Journal of Materials Processing Technology, 110: 61-69.
►Samantaray, D., Mandal, S., Bhaduri, A. K. (2009). *A comparative study on Johnson Cook, modified Zerilli-Armstrong and Arrhenius-type constitutive models to predict elevated temperature flow behaviour in modified 9Cr-1Mo steel.* Computational Materials Science, 47: 568-576.
►Shirakashi, T, Usui, E (1976). *Simulation analysis of orthogonal metal cutting process.* Int. J. Japan Soc. Prec. Eng., 42(5): 340-345.
►Ucun, I, Aslantas, K, Karabulut, A (2009). *Investigation of variation in tool-chip contact length in orthogonal cutting process.* Journal of the Faculty of Engineering & Architecture of Gazi University, 24(3): 477-484.
►Wan Z. P., Liu Y. J., Ye B.Y., et al. (2002). *Study on tool-chip close contact length in metal cutting.* Tool Engineering, 36(4): 8-12.